Recent Advances in Atmospheric, Solar-Terrestrial Physics and Space Weather From a North-South network of scientists [2006-2016]"

PART A: TUTORIAL

Amory-Mazaudier C. [1,2], Menvielle M. [3], Curto J-J. [4], Le Huy M. [5]

[1.] Sorbonne Universités UPMC Paris 06, LPP, Polytechnique, 5 place Jussieu, Paris, France
[2.] T/ICT4D Abdus Salam ICTP, Trieste, Italy
[3.] Université Versailles Saint-Quentin, CNRS/INSU, LATMOS, IPSL, 78280 Guyancourt, France
[4.] Observatorio del Ebro, (OE) CSIC – Universitat Ramon Llull, Roquetes, Spain
[5.] Institute of Geophysics, Vietnam Academy of Science and Technology, Hanoi, Vietnam.

E mail (Christine.amory@lpp.polytechnique.fr).

Abstract This paper reviews scientific advances achieved by a North-South network between 2006 and 2016. These scientific advances concern Solar Terrestrial Physics, Atmospheric Physics and Space Weather. In this part A, we introduce knowledge on the Sun-Earth system. We consider the physical process of the dynamo which is present in the Sun, in the core of the Earth and also in the regions between the Sun and the Earth, the solar wind-magnetosphere and the ionosphere. Equations of plasma physics and Maxwell's equations will be recalled. In the Sun-Earth system there are permanent dynamos (Sun, Earth's core, solar wind - magnetosphere, neutral wind - ionosphere) and non-permanent dynamos that are activated during magnetic storms in the magnetosphere and in the ionosphere. All these dynamos have associated electric currents that affect the variations of the Earth's magnetic field which are easily measurable. That is why a part of the tutorial is also devoted to the magnetic indices which are indicators of the electric currents in the Sun-Earth system. In order to understand some results of the part B, we present some characteristics of the Equatorial region and of the electrodynamics coupling the Auroral and Equatorial regions.

TABLE OF CONTENTS

Introduction

This paper presents the results obtained by a North-South research network. This paper is composed of 2 parts A and B. Part A presents a tutorial and part B the results obtained in the various scientific fields explored.

This network was constituted and structured within the framework of international projects based on the deployment of measurement instruments in non-equipped countries and particularly in Africa. First we will present the main projects and what they have contributed. Then we will introduce the results of this article. It was in Vancouver in 1987 during the symposium of the International Association for Geomagnetism and Aeronomy (IAGA) that the members of the Interdivisional Commission of Developing Countries (ICDC) requested a campaign of measurements on the Equatorial Electrojet be organized. This campaign took place from 1992 to 1994 and named the International Equatorial Electrojet Year (IEEY). At that time there was not yet internet and there was therefore no site dedicated to this experiment. Mazaudier et al., (1993) described the instruments deployed in Africa mainly on West Africa. Amory-Mazaudier et al., (2005) described the results obtained during the IEEY. This project led to the defense of 10 PhD and made it possible to structure the North South research network GIRGEA (Groupe International de Recherche en Géophysique Europe Afrique http://www.girgea.org).

In 2005 the GIRGEA was involved in the International Heliophysical Year (IHY) http://ihy2007.org.

"The IHY project was suggested in 2001 to celebrate the 50th anniversary of the International Geophysical Year (IGY).

''The objectives of IHY 2007 are:

1. – To understand the processes and drivers that affects the terrestrial environment and climate;
2. – To provide a global study of the Sun-Hemisphere system outward to the heliopause;
3. – To foster international cooperation in space science now and in the future;
4. – to communicate the unique scientific results of the IHY to the scientific community and to the public.''
    (Extract from Harrison et al., 2005)

The IHY project promoted the participation of developing nations in the international global studies of the Sun–Earth System. A specific initiative is the ''United Nations Basic Space Science Initiative (UNBSSI) http://wwwoosa.unvienna.org ''. It was based on the tripod concept: instruments, observation and education (Kitamura et al. 2007). Low-cost scientific instruments are deployed all over the world (magnetometers, GPS receivers, radio telescopes, VLF receivers, and others) and particularly in Africa. The most widely deployed instruments in Africa during the IHY project were GPS (Amory-Mazaudier et al., 2009) and magnetometer *www.serc.kyushu-u.ac.jp/magdas/MAGDAS_Project.htm*

The GPS Network deployed over Africa for the IHY combines different networks of GPS receivers:

IGS: http://igscb.jpl.nasa.gov, International Geodesy System,

AMMA: http://www.amma-international.org, Analyse Multidisciplinaire de la MoussonAfricaine,

SCINDA:www.fas.org/spp/military/program/nssrm/initiatives/scinda.htm, Scintillation Network Decision Aid,

As part of the IHY project, the GIRGEA network expanded to Asia and defined a project for Vietnam that led to the defense of 6 PhD (Amory-Mazaudier et al., 2006)

In continuity with IHY project, the International Space Weather Initiative project (http://ww.iswi-secretariat.org), from 2010 to 2012, continued the deployment of scientific instruments in countries requiring measurements and focused research on the impact of solar events on new technologies. In 2012, at the end of the ISWI project, the participants decided that ISWI would now be a research network under the umbrella of United Nations with an annual meeting of the steering committee in Vienna.

The IEEY project has been important because it showed that it was possible to develop high-level research in Africa in less developed areas at the time. The IHY project was fundamental for two points: 1) to globalize the research of the Sun-Earth system, allowing many young scientists to make a career in science and 2) to break the walls between the different disciplines of Sun and Earth physics, so solar physicists and physicists of the magnetosphere, ionosphere and atmosphere had worked and trained together young scientists. The ISWI project brought together fundamental research and applications in particular through the use of Global Navigation Satellite System (GNSS) for research.

This article reviews the results obtained during the various projects presented above. It consists of 2 parts. This first part is a tutorial that presents some knowledge about the Sun-Earth system useful for understanding the results. The second part brings together results on Climate and Atmospheric Sciences, Solar Terrestrial Physics, Space Weather and Capacity Building.

Part A: Tutorial

Introduction

In this section we will present some physical properties and processes of the Sun-Earth system useful for our review. In some areas only a description of morphology will be given with references to useful works to further explore the subject. Our network has been interested in the study of the dynamical and electromagnetic phenomena on a large scale. We will focus on the description of the physical process of the dynamo which allows understanding in a systemic way the solar terrestrial system, and presenting the four main permanent ones: Solar dynamo, Terrestrial core dynamo, Solar-wind magnetosphere dynamo and ionospheric dynamo. We will also present the associated electrical currents and magnetic indices developed to understand this complex system. We will more detail the physics of the ionospheric plasma and of the induction that are useful to understand the equatorial phenomena. Figure 1, from Paterno (2006), summarizes the mechanism of the dynamo that will be used in this section. The starting points are a movement and a magnetic field.

During the last two decades, the physics of the Sun and the solar wind has advanced considerably with the SOHO and ULYSSE satellites. It is now possible when analyzing observations at the level of the Earth to know the state of the Sun using the databases built by solar physicists. As part of the International Heliophysical Year project (IHY), it was possible for ionosphere physicists to familiarize themselves with and use commonly solar data.

1.1 Solar Dynamo

We will only recall here few essential elements necessary for our study; to deepen the subject please consult the site http://solarscience.msf.nasa.gov/dynamo.shtml

It is well known at the present time that the Sun has:
1. a solar magnetic field which has two components: a poloïdal component (~10 G) and a toroidal component (~3-5 kG)
2. That it rotates on itself with a different velocity between the pole (~31 days) and the equator (~27 days) and this differential velocity creates the sunspots (toroïdal magnetic field).

The dipolar component of the solar magnetic field, B_{pol}, is considered as the primary magnetic field, with the motion of the rotating Sun, V_{rot}. Within this magnetic field, it is a dynamo. The discovery of sunspots is attributed to Galileo Galilei and Thomas Hariot around 1610 (Casanovas, 2006). Schwabe (1843) discovered the sunspot cycle (presented on figure 2) and Hale et al., (1919) discovered the poloidal component of the solar magnetic field.

The two components of the solar magnetic field are anti-correlated and they do not produce the same events. The sunspots, which are known for more than 4 centuries, are the main source of the solar flux received on Earth. The poloidal magnetic component acts more on the solar wind. Figure 3 presents the complete solar cycle, at the top panel on the upper and lower edges of the figure we can see the alternation of blue and yellow colors corresponding to the change in the poloidal field direction, every 11 years. At the center of the top panel there is the famous butterfly diagram corresponding to the sunspot cycle. The middle panel shows the variation of the dipole field and the bottom panel the variation of the toroidal field (sunspot cycle). It is observed that the poloïdal field is maximal when the sunspot cycle is at the minimum and vice versa.

Before the International Heliophysical Year, very few physicists of the ionosphere knew the poloidal component of the solar magnetic field. All the studies were conducted with the sunspot cycle which is of course very important for the ionosphere and whose effects are more visible.

We shall see in the remainder of this section how these two components of the solar magnetic field are to be known for our systemic study on Sun Earth system, see the reviews on solar cycle and geomagnetic activity by Legrand and Simon (1989) and Simon and Legrand (1989).
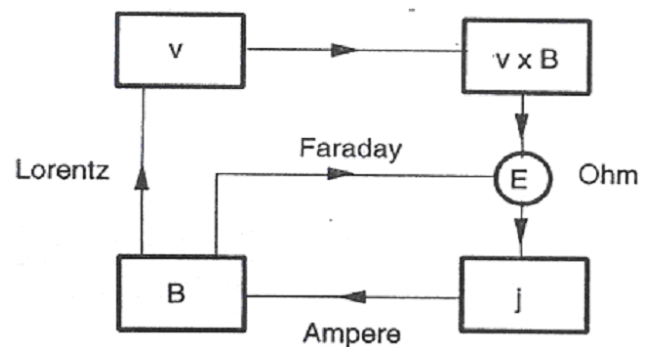
Figure 1: Schematic representation between plasma motion and magnetic field [after Paterno, 2006]. Comments by Paterno 'A motion v across a magnetic field B induces an electric field vxB, which produces an electric current J=σ (E + v×B) via Ohm's law where σ is the electric conductivity and E an electric field. This current produces in turn a magnetic field $\nabla \times B = \mu J$, where μ is the permeability. The magnetic field creates both electric field E through Faraday's law $\nabla E = -\delta B / \delta t$ and Lorentz force J×B which reacts on the motion v.

Figure 2 : Sunspot cycle

Figure 3 : Top panel: the magnetic butterfly diagram in grey scale (the original figure is by D.H. Hathaway, NASA/MSFC), where white (black) represents p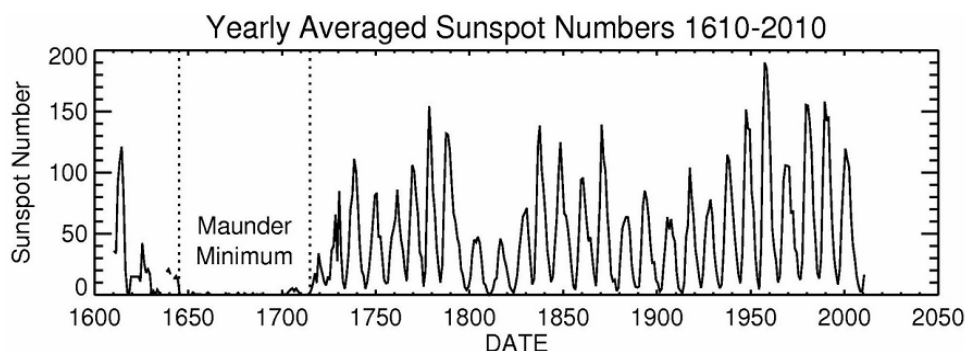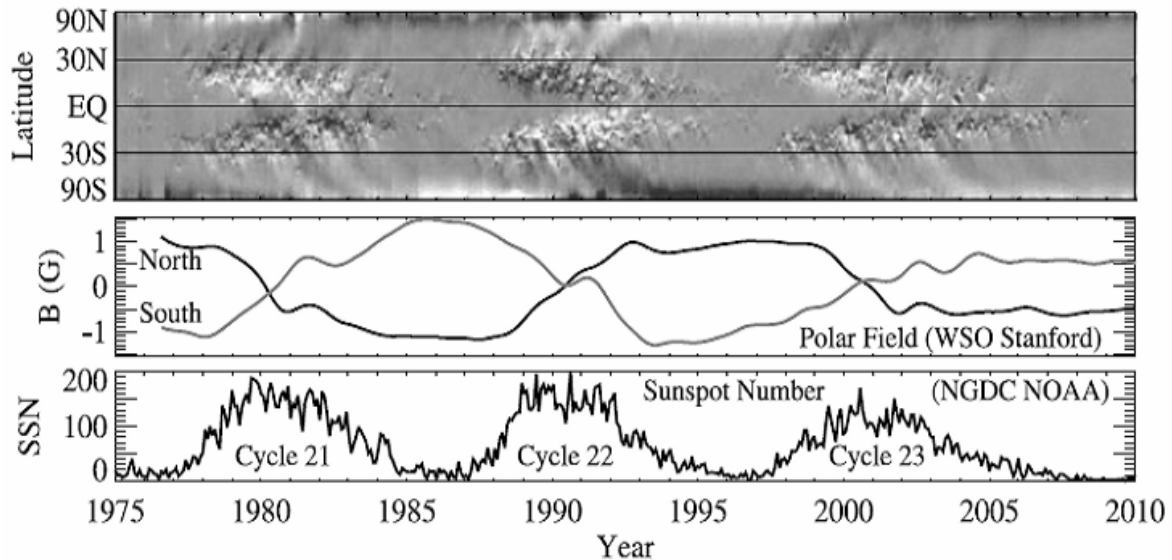ositive (negative) field; Middle panel: solar polar region field (between $\pm 55^0$ and the poles) observed by Wilcox Solar Observatory (WSO) at Stanford; bottom panel: sunspot number of the same three cycles 21 to 23 using data from NOAA NGDC. The poloidal field of bipolar MCs shows a cyclic reversal of the same periodicity with the solar magnetic cycle, (Li et al., 2011)

1.2 Terrestrial Core Dynamo

The Earth's magnetic field can be thought of as a huge cocoon, protecting the Earth planetary surface from cosmic radiation and solar wind charged particles bombardment. Without it, life as we know it would not exist.

About 94% of the total Earth's magnetic field, the so-called main field is generated by the terrestrial core dynamo. The remaining 6% corresponds partly to the time varying magnetic signature of electrical currents generated by the solar-wind magnetosphere and ionospheric dynamos, and partly to the signature of the magnetization of geological materials in the lithosphere – the rigid outer part of Earth, consisting of the crust and upper mantle. This magnetization corresponds either to the fossilization of the geomagnetic field at the time of deposition of geological materials (remanent magnetization), or results in the amplification of the present geomagnetic field (induced magnetization);

In this section, we briefly recall basics on the terrestrial core dynamo, responsible for the main field. Its intensity is in the range of 30,000 to 60,000nT at the Earth surface, and its time

Figure 4 : The core dynamo: Horizontal intensity H (nT) at 2010.0 from IGRF model (IGRF-11 model), middle panel Inclination I (degree) and bottom panel: total intensity F (from Macmillan and Finlay, 2011)

variations have periods in the range of few years to hundreds of millions of years, the low period cut-off resulting from electromagnetic field filtering by the conductive mantle.

It is generated at depths greater than 3000 km by a self-sustaining dynamo associated to the convection movement of molten very conductive materials – mostly iron – in the outer liquid core. This movement is driven by the cooling of the planet that results in convective motions associated to heat transfer from the center of the planet outwards on the one hand, and to upwards motion of light materials released by core materials crystallization at the surface of the inner solid core on the other hand. It satisfies Maxwell's (electromagnetic field) and Navier-Stockes's (core material convection) equations, coupled through the Lorentz force, i.e. the force exerted on conductive material moving through magnetic field force lines. It is now well accepted that the outer core tangential flow results from the geostrophic balance between the Coriolis force and the force of the pressure gradient, for the time scales of the historical secular variation, can be considered as-geostrophic. The analysis of the main field and of its secular variation makes it possible to get information on the motions at the surface of the outer liquid core, and on its evolution since the beginning of systematic observations at the end of the nineteenth century.

The magnetic field is fully described by an appropriate set of three elements selected from: Northerly intensity, X, the Easterly intensity, Y, and the vertical intensity, Z (geographical axis); the horizontal intensity, H, the total intensity, F, the inclination angle, I, measured from the horizontal plane to the field vector, positive downwards, and the declination angle, D, measured clockwise from true North to the horizontal component of the field vector. The magnetic equator corresponds to the points where I=0.

Outside the conductive Earth, the main field of internal origin is the negative gradient of a magnetic potential V that satisfies the Laplace's equation. This potential, and accordingly the elements of the main magnetic field, can be described in terms of a sum of spherical harmonics which each satisfy Laplace equation. This is, in particular, the case of the International Geomagnetic Reference Field (IGRF) that is an internationally agreed and widely used mathematical model of the Earth's magnetic field of internal origin. Each constituent model of the IGRF is a set of spherical harmonics of degree n and order m, each of them being associated to a Gauss coefficient. The higher the degree n is, the smaller the spatial wavelength and the more rapid the decreasing with the distance to the Earth is. Spherical harmonics developments are the generalization to spherical geometry of Fourier development in 2-D situations.
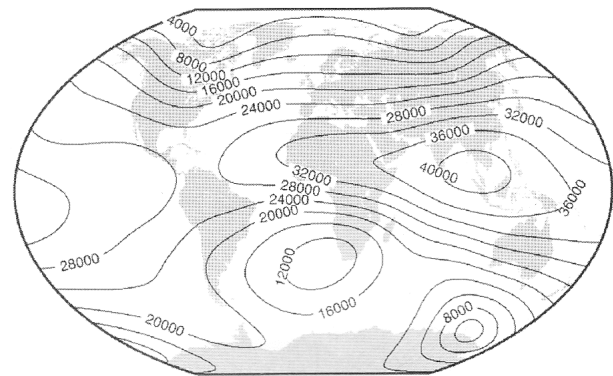
The first IGRF has been ratified by the International Association of Geomagnetism and Aeronomy (IAGA) in 1969, and has been revised and updated every five years since then. The constituent of the IGRF models extend to spherical harmonic degree 10 up to and including epoch 1995.0; thereafter they extend to degree 13 to take advantage of the availability of excellent satellite data (see Macmillan and Finlay (2011), and reference therein for further details). Figure 4 presents global maps of selected magnetic elements, based on IGRF for 2010.0.

The order n=1 IGRF Gauss coefficients are at least ten time larger than those for orders n>1. The n=1 component corresponds to the so-called dipolar field that would be generated by a magnet located at the center of the Earth, and tilted with respect to the Earth's rotation axis. Since, in addition, the n=1 component is the one with the slowest decay with distance to the Earth's centre, the Earth's magnetic field can be properly approximated by the n=1 IGRF dipolar field.
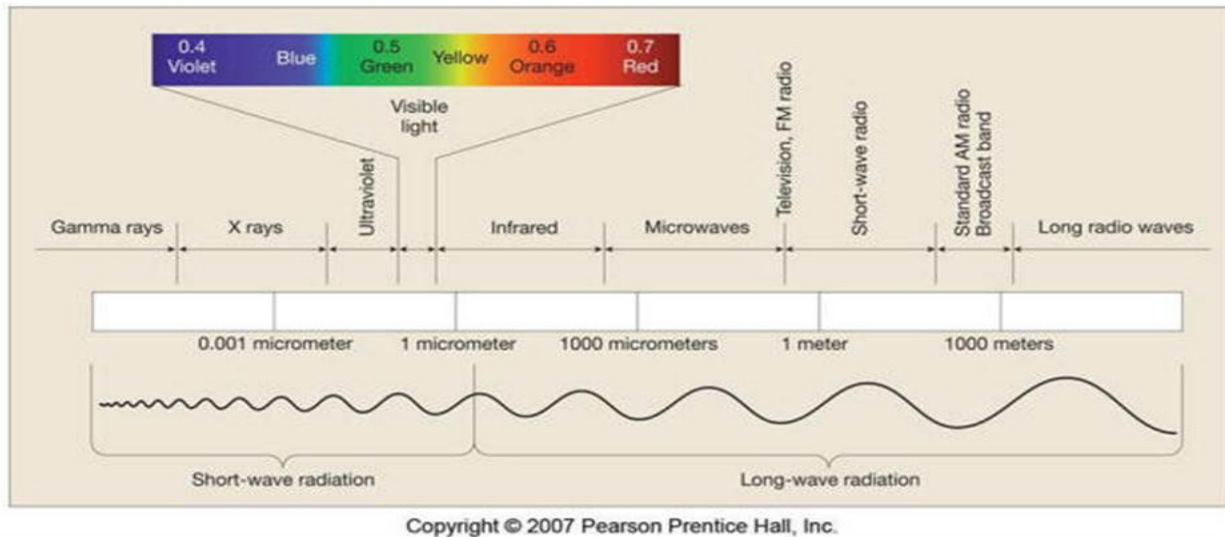

Figure 5 : Solar radiations

1.3 Sun-Earth's Connections

1.3.1 Regular radiations

The Sun emits continuously many radiations, which are shown in figure 5. The UV, EUV and X radiations are the primary source of the ionosphere by the photo ionization.

1.3.2 Regular solar wind

Figure 6 shows the solar wind, which compresses the magnetosphere (cavity of the earth's magnetic field), at the front and stretches it at the rear. The regular solar wind is a constant stream of coronal material that flows off the Sun at a speed of about 300-400km/s. It consists of mostly electrons, protons and alpha particles with energies usually between 1.5 and 10 KeV. The Earth's magnetic field acts as a shield for solar wind. However, there are regions of the ionosphere that are directly connected with the interplanetary medium and this the solar wind flow. The solar wind carries part of the solar magnetic field towards the Earth. The magnetic field in the solar wind is called interplanetary magnetic field (IMF).
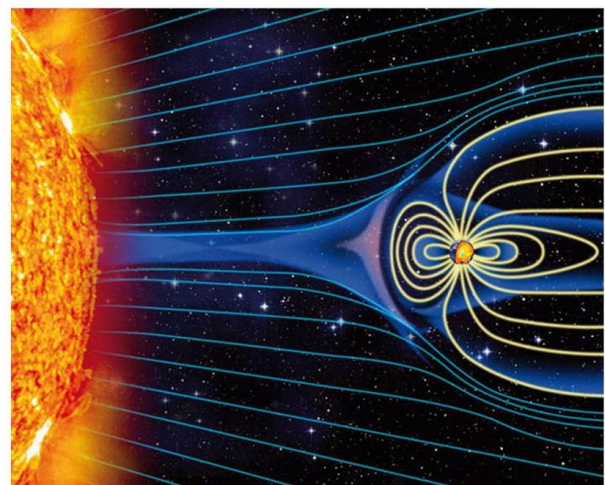

Figure 6 : Solar wind source (Amory-Mazaudier et al., 2017)

1.3.3 Solar disturbances related to radiations (solar flare, solar burst…)

A solar flare occurs when magnetic energy that has built up in the solar atmosphere is suddenly released. Radiation is emitted across virtually the entire electromagnetic spectrum, from radio waves at the long wavelength end, through optical emission to x-rays and gamma rays at the short wavelength end. The solar flare reaches the earth in 8 minutes (speed of the light), there is no interaction with magnetosphere. The ionizing radiations of the solar flare (X, UV, EUV) create a strong increase of the ionospheric ionization and disturb the Global Navigation Satellite System by adding a delay. Figure 7 shows a picture of a Solar Flare and figure 8 shows its effect in the Earth's environment. In the E layer the solar flare increases the electric conductivity and as a consequence increases ionospheric electric currents (section 3 of tutorial) and the Earth's magnetic field associated to these ionospheric electric currents (section 4 of tutorial). The signature of the solar flare on the magnetic field is visible and is called a crochet, see Curto et al., (1994a, 1994b).

Figure 7 : Solar Flare (SOHO data) (Amory-Mazaudier et al., 2017)

1.3.4 Solar disturbances affecting the solar wind (CME, HSSW, CIR …)

The Coronal Mass Ejections (CMEs) are due to powerful magnetic explosions in the Sun's crown, which project the ionized plasma into the interplanetary space, and the associated neutral gas by collision. The CMEs carry billions of tons of material. The relaxation of the plasma, initially compressed by the high pressures existing on the surface of the Sun, increases its volume to a greater extent than that of the Sun in the relatively dense interplanetary space. A gigantic plasma bubble moves away at supersonic speed from the Sun at over 300,000 km / h, opening the lines of force of the solar magnetic field. At its arrival in the vicinity of the Earth after three to four days, the gigantic plasma bubble interacts with the Earth's magnetic field, and produces northern and southern lights, geomagnetic storms, disrupts radio communications, satellites and electricity distribution systems. Figure 9a illustrates the phenomena of CME. Occurrence of CME is maximal with the maximum sunspot cycle, see Gopalswamy (2010).

HSSW, CIR: High-speed solar-wind streams flow from solar coronal holes; the fast solar wind interacts with slow wind streams producing regions of enhanced magnetic field strength and particle density that are known as co-rotating interaction regions. Figure 9b, from Legrand (1984), illustrates the solar wind flow from a coronal hole, in black on the figure. The coronal holes are recurrent and occur

Figure 8 : Effect of a solar flare on GNSS signal (Amory-Mazaudier et al., 2017)

near sunspot minimum when the poloïdal component of the solar magnetic field is maximal. HSSW can last for several days and input as much energy as a storm driven by a coronal mass ejection (Kavanagh and Denton, 2007). The occurrence of fast solar winds is maximal during the descending phase and the minimum phase of the sunspot cycle

In this section we have presented some definitions concerning the main solar events affecting the solar wind, which are the CME and the HSSW. CME and HSWW may be causing magnetic storms that severely disrupt the terrestrial environment. Gonzales et al., (1994) have defined criteria for classifying magnetic storms based on solar wind parameters and the magnetic index Dst which will be presented in the magnetic indices section.

In the work presented in Part 3 'Solar Terrestrial Physics' and Part 4 'Space Weather' we have systematically used solar databases such as the LASCO catalog on the CME (https://cdaw.gsfc.nasa.gov/CME_list/), to develop case studies.
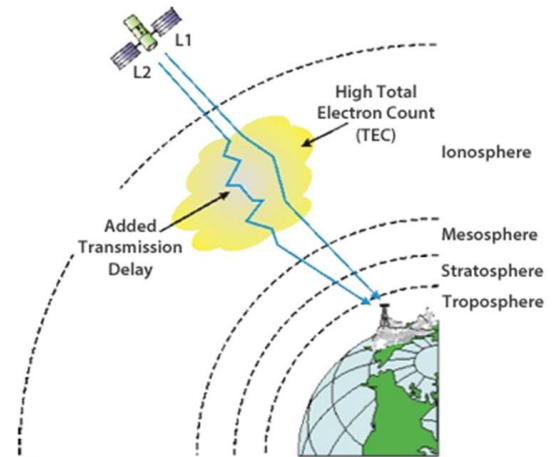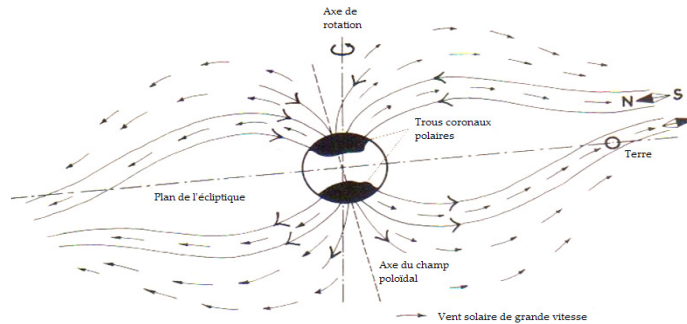

a   b

Figure 9: CME and HSSW, a) A CME starting from the Sun and arriving near the Earth and b) Coronal holes in black with (from Legrand 1984)

1.4 Ionosphere and Atmosphere

Figure 10 from Rishbeth and Gariott (1969), on the left side, presents the different layers of the Atmosphere and on the right side the different layers of the Ionosphere. The layers of the atmosphere are defined by changes in the gradient of temperature. The Troposphere 0- 11 km is the region where meteorological phenomena take place. The Stratosphere 11- 30 km is a region of high turbulence. The mesosphere 30-80 km is the region where the solar UV radiation is completely absorbed by ozone. Finally the thermosphere 80- 600 km is strongly ionized by the X and EUV solar radiations. Above 600 km there is the exosphere which is a region where the collisions are infrequent and where the particles follow ballistic orbits and are governed only by the electromagnetic forces.

The Ionosphere is the ionized part of the atmosphere due to the absorption of the UV, EUV and X radiations It is organized in different layers of altitude called D, E, F1 and F2.

Region D is between 50 and 90 km and coincides with the mesosphere. Its ionization is due to the ionization of nitrogen monoxide (NO) by solar UV radiation, X-rays and, essentially at night, the capture of an electron by oxygen molecules O_2. The layer D is thus

composed of positive ions NO +, negative ions O_2^- (mainly at night) and electrons. In fact, these ions evolve in part by the formation of aggregates gathering the original ions and water molecules.

The E layer, located between 90 and 150 km, comes from the ionization of the oxygen molecule (O_2) and the molecule of nitrogen (N_2) by the EUV photons and, to a lesser extent, by the X-rays. Layer E disappears rapidly at night, the density decreasing by 2 or 3 orders of magnitude, except when the high-altitude structure of the neutral winds leads to the formation of sporadic E-layers from meteoric ions and (ii) at high latitude where the auroral activity and the precipitation of energetic electrons maintain high densities. In the E layer, electric currents are created by dynamo effect of the atmosphere.
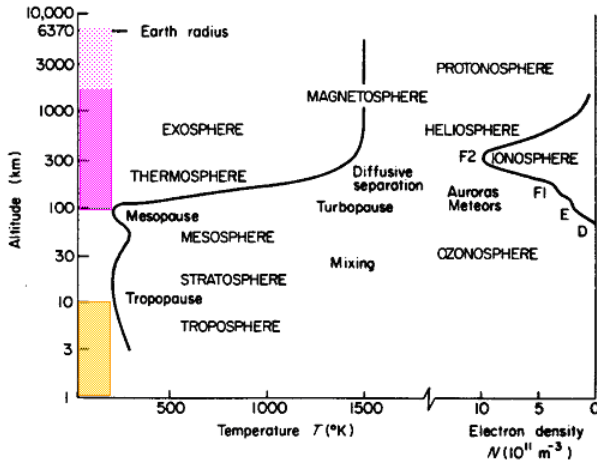

Figure 10 : Ionosphere and Atmosphere after [Rishbeth and Gariott, 1969]

The Region F, created mainly by EUV radiation, extends from 150km to the exosphere. During the day, it has two layers (F1 and F2). The layer F1 is situated between 150 and 200 km approximately. The layer F2 extends beyond 200 km and in the exosphere and is the only one to survive at night, due on the one hand to the long time constants of the reactions that control the losses of ions and electrons. On the other hand, the transport of the plasma along the force tubes of the earth's magnetic field which partially empty the magnetospheric reservoir in favor of the higher ionosphere.

The equation of continuity gives the rate o change of electron concentration as the sum of the gain by production (q) minus the loss by destruction l(N)and minus the change by transport div (NV) as we consider that the transport processes results in a net drift velocity.

$$\frac{\partial N}{\partial t} = q - l(N) - div(NV) \tag{1}$$

1.5 Ionospheric dynamo and its associated electric current systems

1.5.1 Ionospheric dynamo

We consider a stationary regime to write the equation of motion in the form:

$$F = m\vec{g} = m\frac{d\vec{V}_r}{dt} = 0 \tag{2}$$

This gives the following two equations for each species (i) of ions and (e) for the electrons:

$$0 = m_i g - \frac{1}{N_i}\nabla\left(N_i kT_i\right) + e\left(E + V_i \times B\right) - m_i \nu_{in}\left(V_i - V_n\right) - m_e \nu_{ei}\left(V_i - V_e\right) \tag{3a}$$

$$0 = m_e g - \frac{1}{N_e}\nabla\left(N_e kT_e\right) - e\left(E + V_e \times B\right) - m_e \nu_{en}\left(V_e - V_n\right) - m_e \nu_{ei}\left(V_e - V_i\right) \tag{3b}$$

In these equations, the physical meaning of the various terms is as follows:

- Force of gravity: $\vec{P} = m\vec{g}$,

- Force of pressure: $\vec{F}_p = \frac{1}{N}\vec{\nabla}(NkT)$

N and T are respectively the concentration and the temperature of the charged particle

- Force of Lorentz: $\vec{F}_{en} = \pm e(\vec{E} + \vec{V}_n \times \vec{B})$

Where e is the elementary charge, the sign "+" for the positive ions and the sign "-" for the electrons, and $\vec{B}$ and $\vec{E}$ are the electric field and magnetic field vectors.

- Collision forces: $\vec{F}_c = m_i \nu_{in}\left(\vec{V}_i - \vec{V}_n\right)$ or $m_e \nu_{ei}\left(\vec{V}_i - \vec{V}_e\right)$ or $m_e \nu_{en}\left(\vec{V}_e - \vec{V}_n\right)$ or $m_e \nu_{ei}\left(\vec{V}_e - \vec{V}_i\right)$

Express the effect of collisions with neutral particles and ions (ni) and electron (ne) or between ions and electrons (ie), m is the mass and velocity of the charged particle, ν the collision frequency between a charged particles with the neutrals (n) or other charged particle.

In the perpendicular direction to the Earth's magnetic field and below the altitude of ~160km, gravity and pressure gradients can be neglected in front of the other forces. The equations of motion for ions and electrons are reduced to:

$$e\left(\vec{E} + \vec{V}_{i\perp} \times \vec{B}\right) = m_i \nu_{in}\left(\vec{V}_{i\perp} - \vec{V}_{n\perp}\right) \tag{4}$$

$$e\left(\vec{E} + \vec{V}_{e\perp} \times \vec{B}\right) = 0 \tag{5}$$

In the perpendicular direction, the neutral atmosphere drives the ions through the lines of the Earth's magnetic field and thus creates a differential velocity between the ions and the electrons and as a consequence electric currents.
The expression of the electric current density is :

$$\vec{J} = N_e e\left(\vec{V_i} - \vec{V_e}\right) \tag{6}$$

7

It can be expressed also as:

$$\vec{J} = \overline{\overline{\sigma}}\left(\vec{E} + \vec{V_n} \times \vec{B}\right) \qquad (7)$$

Where $\overline{\overline{\sigma}}$ is the conductivity tensor, $\vec{E}$ the electrostatic electric Field, $\vec{V_n}$ the neutral wind and $\vec{B}$ the terrestrial magnetic field. It is important to recall here that the absorption of the UV solar radiation in the mesosphere produces the atmospheric tides which propagate from the middle atmosphere to the E region and which are an important component of the motions of the neutral atmosphere $\vec{V_n}$ in the E dynamo region. Figure 11, from Evans (1978), presents the mechanism of propagation of migrating atmospheric tides generated in the Stratosphere (Chapman and Lindzen, 1970). In addition to migrating atmospheric tides, there are non-migrating tides generated by atmospheric convection in the troposphere (Hagan and Forbes, 2002; Hagan and Forbes, 2003) which also influence atmospheric movements at the altitudes of the dynamo E region of the Ionosphere.

In the F region (above 160 km), the motions of the ions and electrons in the perpendicular direction to $\vec{B}$ are equal and are only due to the Lorentz force $\vec{V_t} = \vec{V_e} = \frac{\vec{E} \times \vec{B}}{B^2}$.

In the direction parallel to the Earth's magnetic field, the equations of motions for the ions and the electrons are :

$$0 = m_i g - \frac{1}{N_i}\nabla\left(N_i k T_i\right) - m_i \nu_{in}\left(V_{i//} - V_{n//}\right) = V_{n//} + V_{d//} \qquad (8)$$

$$0 = m_e g - \frac{1}{N_e}\nabla\left(N_e k T_e\right) - eE_{//} - m_e \nu_{en}\left(V_{e//} - V_{n//}\right) = V_{n//} + V_{d//} - \frac{J_{//}}{N_e e} \qquad (9)$$

Where $V_{n//}$ is the atmospheric motion , $V_{d//}$ is the velocity of ambipolar diffusion under the influence of pressure gradient and gravity , $\vec{J_{//}}$ the current parallel to the lines of the magnetic field, Ne Is the density of the electrons and e is the charge of the electron. Below 180 km, the ambipolar diffusion velocity can be neglected.

The ionospheric electric currents flowing in the E layer (100-150km) are at the origin of the regular variations of the Earth's magnetic field: to deepen the subject please read Richmond (1995).

The ionospheric electric currents (Ampere's law) produce ground magnetic field variations and these ground magnetic variations are used to determine 'Equivalent electric current system'. We speak of equivalent electric currents because these currents are deduced by inversion of the terrestrial magnetic field data and this requires a model for the circulation of the electric currents.
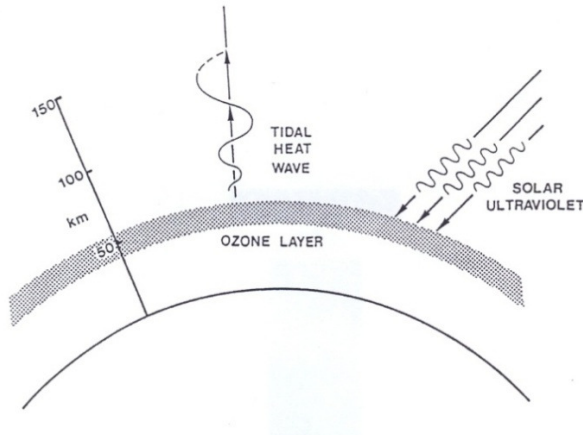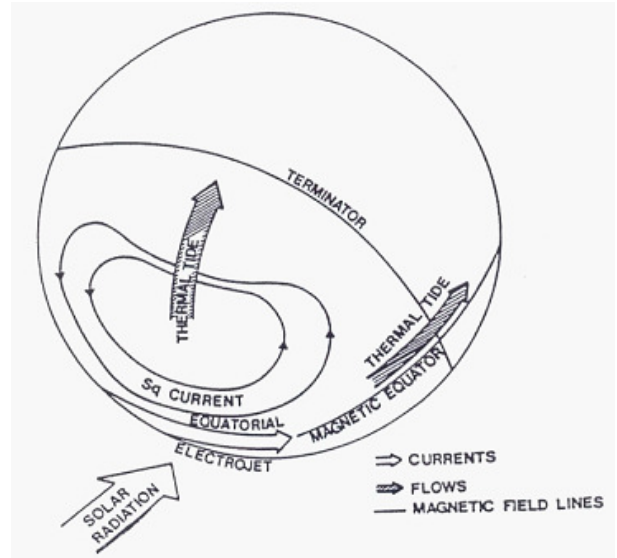

Figure 11 : Atmospheric tides (Evans 1978

Figure 12 : Equivalent electric currents Sq and EEJ

1.5.2 Sq and EEJ

The ionospheric dynamo has two associated equivalent electric current systems which are: 1) the Sq current system (Chapman and Bartels 1940) and 2) the Equatorial Electrojet EEJ (Chapman 1951).

For the Sq equivalent current system, one considers that the currents circulate in an infinite plane layer above a flat earth. For the EEJ current it is assumed that the current model is a ribbon. Figure 12 shows the equivalent electrical currents Sq and EEJ. These currents linked to the existence of the E region circulate on daylight side of the earth.

1.5.3 The inospheric currents induce currents in the Earth

The ionospheric currents associated to the equatorial electrojet, hereafter denoted as $S_R{}^E$, can be roughly modeled in the dayside hemisphere by a quasi-linear concentration of currents flowing in the ionospheric E-layer along the dip equator. In order to ensure the divergence free condition for these currents, closing currents should exist, making it essential to deal with these currents when studying the induction phenomena associated with the equatorial electrojet.

1.5.3a The Maxwell's equations

Let be the magnetic induction related to the ionospheric $S_R E$ currents, B_i be the magnetic induction related to the induced currents that flow in the conducting solid Earth, and B be the total induction. $\vec{B} = \vec{B_i} + \vec{B_e}$ satisfies Maxwell's equations:

$$\vec{\nabla} \times \vec{B} = \mu \vec{J} \tag{10a}$$

$$\vec{\nabla} \times \vec{E} = -\frac{\partial \vec{B}}{\partial t} \tag{10b}$$

$$\vec{J} = \sigma\left(\vec{E} + \vec{v} \times \vec{B}\right) \tag{10c}$$

$$\vec{\nabla}.\vec{B} = 0 \tag{10d}$$

$$\vec{\nabla}.\vec{J} = 0 \tag{10e}$$

where $\vec{E}$ is the electric field, $\vec{J}$ the density of volume current, and $\vec{v}$ the linear speed of rotation of the Earth at the equator. $\quad$ is the electrical conductivity of the medium, and μ its magnetic permeability, which we assume to be uniform and equal to that of a vacuum. The space is referred to an Oxyz Cartesian frame defined with respect to the Sun, where Ox and Oy are horizontal axes positive northwards and eastwards respectively, and Oz the vertical axis positive downwards.

Consider the case of homogeneous conductive domains. Taking the curl of equation (10a) and substituting (10b) and (10c), gives:

$$\nabla^2 B = \mu\sigma\left(\frac{\partial B}{\partial t} - \nabla \times (v \times B)\right) \tag{11a}$$

Similarly, taking the curl of equation (10b) and substituting (10a) and (10c) leads to:

$$\nabla^2 E = \mu\sigma\left(\frac{\partial E}{\partial t} + \frac{\partial}{\partial t}(v \times B)\right) \tag{11b}$$

1.5.3b Induction by the diurnal variation

The $S_R{}^E$ currents can be described as a system of constant intensity and fixed geometry. Such a model provides a relevant first-order model for studying induction at equatorial latitudes, since the $S_R{}^E$ day-to-day variability can be neglected in such studies, except perhaps at times close to local noontime (see, e. g., Ducruix et al., 1977; Vassal et al., 1998).

In this limiting case, $\partial\vec{B}/\partial t$ and $\partial\vec{E}/\partial t$ are zero, and the Earth rotates below a current system that is fixed with respect to the Sun. The linear speed of rotation of the Earth, $\vec{v}$, lies along the **y** axis and:

$$\nabla \times (v \times B) = -v\frac{\partial B}{\partial t} \tag{12}$$

Where $v = |\vec{v}|$. Consequently, the source term for the induction reduces to $\mu\sigma v\frac{\partial \vec{B}}{\partial t}$ in equations (11a) and (11b).

Equations (11a) and (11b) then reduce to:

$$\nabla^2 B = -\mu\sigma \cdot \nabla x(v \times B) \tag{13a}$$

$$\nabla^2 \vec{E} = 0 \tag{13b}$$

Induced electric fields are therefore the signature of magnetic induction $\vec{B}$ gradients in the east-west direction. They are consequently expected to be negligible, if not zero, close to the noon meridian where $\partial[\mathbf{y}\times(\mathbf{B}\times\mathbf{y})] / \partial y \approx 0$, and are likely to be the signature of closing currents which are, in fact, associated with **B** gradients in the y direction. Furthermore, the differential operators present in the equations (13a), (13b), and (11a) only involve derivatives with respect to space. The magnetic induction, $\vec{B}$, and the induced electric field, $\vec{E}$, therefore have the same time dependence. Moreover, since $\vec{B}_i << \vec{B}_e$ (Ducruix et al., 1977), the ionospheric $S_R{}^E$ currents together with the related magnetic and induced electric currents variations have the same time dependence during a given day. All of these variations would then have the same day-to-day variability.

Ducruix et al. (1977) made numerical simulations with a model that is oversimplified and probably not very realistic as far as the geometry of the ionospheric return currents is considered. Their results gave a clear numerical confirmation of the two basic results we deduced from the Maxwell equation: that the induced electric fields correspond to the east-west gradient in the magnetic field, and that their intensity is proportional to that of the magnetic SRE variation.

1.5.3c Induction by the irregular variations

During disturbed magnetic situations, the ionospheric currents flowing in the electrojet and related to the irregular magnetic disturbances, are homogeneous over a wide range of longitudes and fluctuate temporally with time constants in the order of a few minutes to a few tens of minutes. The source term related to $\vec{\nabla}x(\vec{v}x\vec{B})$ is then negligible compared to that related to $\partial\vec{B}/\partial t$, and, as a first approximation, one can consider that the current system does not move with respect to the Earth. Equations (13a) and (13b) then reduce to the classical induction equations for a conductive body in a time-varying electromagnetic field:

$$\nabla^2\vec{B} = \mu\sigma\frac{\partial\vec{B}}{\partial t} \tag{14a}$$

$$\nabla^2\vec{E} = \mu\sigma\frac{\partial\vec{E}}{\partial t} \tag{14b}$$

At night time, the Tikhonov-Cagniard's plane wave approximation holds, and so does the magnetotelluric interpretation.

During daytime, however, the equatorial electrojet exercises considerable control over the transient electromagnetic field at the Earth's surface. Given the latitudinal extent of the equatorial electrojet (see e.g., Fambitakoye and Mayaud, 1976; Doumouya et al.,

1997), the plane wave approximation no longer holds for frequencies smaller than a few cph, such that interpreting daytime electromagnetic observations must take into account the actual distribution of ionospheric currents at equatorial latitudes.

The variation of the E-W current density with latitude has been studied for decades. Surface magnetic data clearly shows that the equatorial electrojet ionospheric equivalent currents are symmetrical with respect to the center of the jet. Various symmetrical models of distributions of ionospheric equivalent currents have been proposed:

a 1-dimensional symmetrical distribution of E-W ionospheric currents scaled by its latitudinal extent and its intensity at the center:

$$I(x) = I_0 (1 - x^2 / a_p^2)^m \qquad (15a)$$

where I_0 is the current density at the center of the electrojet, ap the 'half-width' of the electrojet and x the distance to the center of the electrojet. Chapman (1951) considered uniform (m = 0) and parabolic (m = 1) distributions of current. Fambitakoye (1976) showed that quadratic models (m = 2) account fairly accurately for the magnetic effects observed at the Earth's surface. Fambitakoye and Mayaud (1976), and then Doumouya et al. (1997) used this latter model to characterize the day-to-day and seasonal variability of the equatorial electrojet and found that ap was of the order of 300 km.

a cosine distribution with 'half-period' ac: (Hutton, 1972)

$$I(x)/I_0 = \cos(2x/a_c) \qquad (15b)$$

a gaussian distribution scaled by a 'standard deviation' ag (Peltier and Hermance, 1971)

$$I(x)/I_0 = \exp(-x^2 / 2a_g^2) \qquad (15c)$$

These three distributions do not differ significantly when they are close to the center of the electrojet, provided the a_p, a_c, and a_g values are consistent. With a realistic 300 km a_p value and appropriate a_c (320 km) and a_g (140 km) values, the calculated error remains less than 10 per cent for distances to the center of the jet less than 250 km (see e. g., Vassal et al., 1998).

The cosine model corresponds to ionospheric currents extending towards infinity in the N-S direction, and therefore does not account for the effects of the limited latitudinal extent of the equatorial electrojet. In contrast, the polynomial and gaussian models correspond to ionospheric currents of limited latitudinal extent, and are therefore likely to provide more realistic models of the electromagnetic field associated with the equatorial electrojet.

Peltier and Hermance (1971) solved the induction problem for gaussian distributions of currents. Vassal et al. (1998) and Luu Viet et al., (2014a) (see Part B section 2.8) used their results to study the electromagnetic field for a realistic gaussian electrojet above a stratified conductive medium. Their results showed that the equatorial electrojet gives rise to a source effect in the magnetotelluric impedance that depends both on the distance to the center of the electrojet and on the distribution of conductivity in the crust
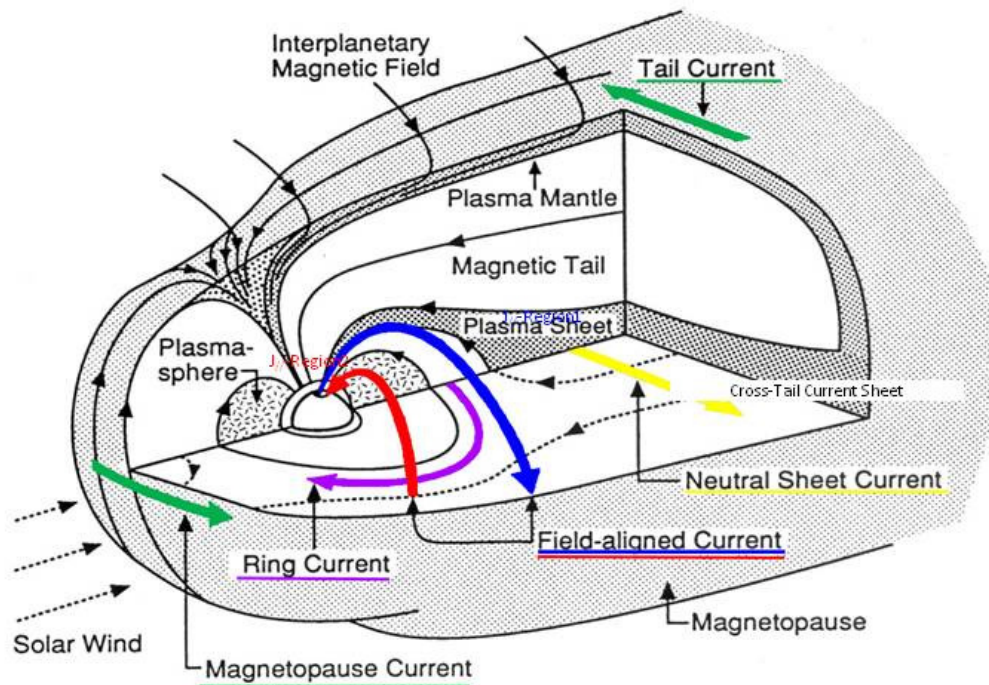

Figure 13: the magnetosphere and the electric current systems in the magnetosphere

1.6 Solar wind magnetosphere dynamo and its associated electric current systems

1.6.1 The solar wind-magnetosphere dynamo

The solar wind magnetosphere dynamo converts the movement of the solar wind into electrical energy transmitted to the magnetosphere. Two main physical processes are invoked for this transfer: 1)   the viscous interaction between solar wind and magnetosphere (Axford and Hines, 1961) and 2) magnetic reconnection (Dungey, 1961), this second mechanism is much more effective than the first mechanism.

The interplanetary electric field $\vec{E_i}$ is given by the following expression:

$$\vec{E_i} = -\vec{V_{sw}} \times \vec{B_{imf}}$$

(16)

Where $\vec{V_{sw}}$ the solar wind and $\vec{B_{imf}}$ the interplanetary magnetic field.

1.6.2 Solar wind magnetosphere dynamoand its associated electric current systems in the magnetosphere

Figure 13 presents the topology of electric currents in the magnetosphere associated to this dynamo. There are the currents flowing on the magnetopause at the front of the magnetosphere which are also called Chapman Ferraro currents. There are currents flowing in the equatorial plane of the magnetosphere at a distance of few terrestrial radius called ring current. There are currents in the tail of the magnetosphere and finally the electrical currents aligned along the terrestrial magnetic field also called Birkeland currents. The Chapman Ferraro electric currents circulate in the magnetopause which is a layer between the solar wind and the terrestrial magnetic field. In this region the pressure of the geomagnetic field is balanced by the dynamic pressure of the solar wind (Chapman and Ferraro, 1931). The ring current is driven by gradient and curvature drifts in the plasma sheet, with an additional contribution from the magnetic moments of all the particles. The ring current keeps the pressure gradient and the Lorentz Force in balance. In the magnetosphere the movement of the particles which is converted into ring current is a temporary dynamo internal to the magnetosphere existing during geomagnetic activity. It was Störmer (1907, 1911 , 1913), at the beginning of the second century, who first studied the trajectories of particles and the formation of the ring current under the action of the earth's magnetic field. Akasofu (1972) proposed that the tail currents flowing at the boundary of the plasma sheet are disrupted and deflected toward the Earth on the evening side. These currents via Birkeland (field aligned current) be converted to a westward electrojet. The field aligned currents proposed by Birkeland (1908, 1913). These currents connect the magnetospheric electric currents to the ionospheric electric currents. The closure of the magnetospheric current loops requires fields aligned currents flowing into and out the ionosphere. The field aligned current were detected by satellite by Amstrong and Zmuda (1970).
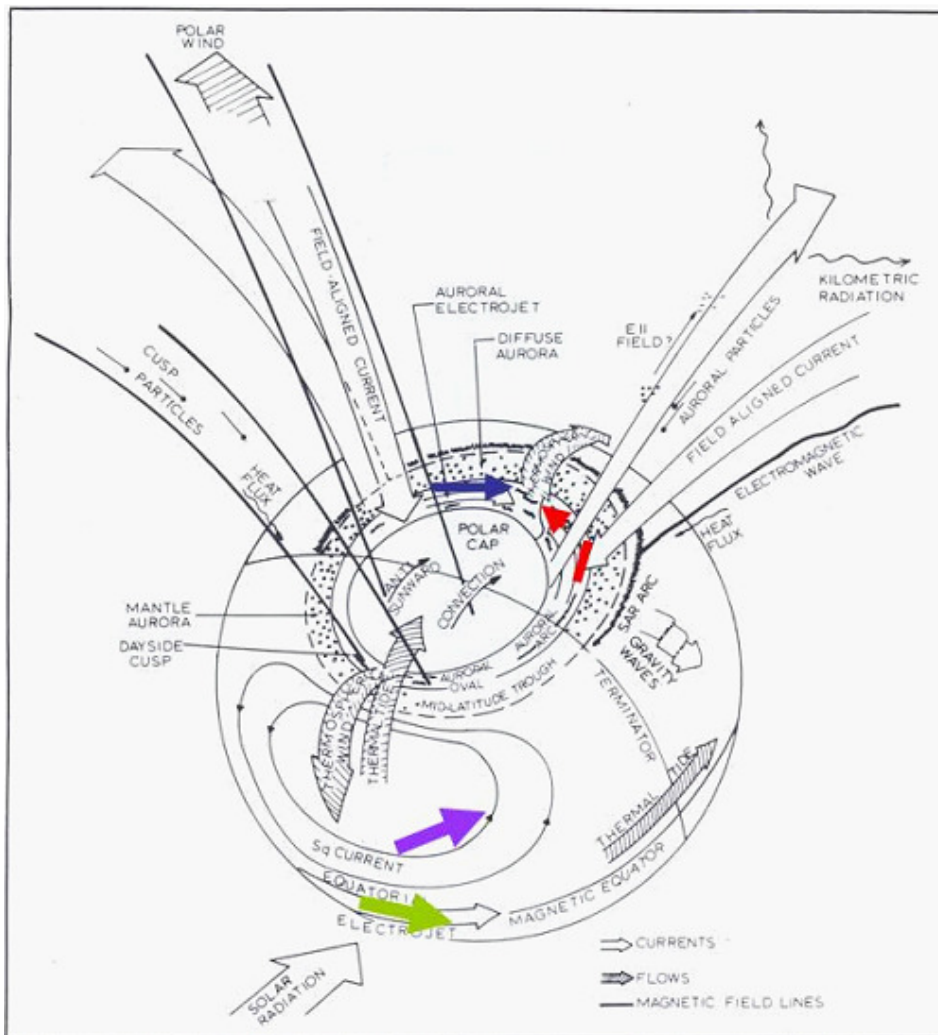
Figure 14 : Ionospheric electric currents

1.6.3 Solar wind magnetosphere dynamo and its associated electric current systems in the ionosphere

The auroral zone is a complex area from the point of view of dynamics and electromagnetism. It is a zone of coupling between the interplanetary medium, the magnetosphere, the thermosphere and the ionosphere. Figure 14 presents the most important parameters at high latitudes:

1) the field aligned currents closing in the E region of the Ionosphere
2) the magnetospheric convection electric field transmitted to the auroral ionosphere via the lines of the magnetic field
3) the precipitation of particles increasing the ionospheric conductivities in the auroral zone,

as a consequence there are strong electric currents flowing in the E region of the ionosphere. These currents are called auroral electrojets.

In turn, these strong electric currents transmit impulse $\vec{J} \times \vec{B}$ and heat to the auroral atmosphere through Joule heating $Q = \vec{j} . \vec{E}$

and create a thermal expansion of the atmosphere and disturbances in the circulation of the thermospheric winds.

As our studies concern more the equatorial zone, we will present the physical processes of the auroral zone influencing the low latitudes in the paragraph 1.8.4.: Electrodynamics coupling between the high and low latitudes.

1.7 The magnetic indices

1.7.1 Magnetically quiet and very quiet 24-hour and 48-hour intervals

Two activity classifications of days are currently used.

The first one aims at identifying the *quietest* and *most disturbed* days of the month. It was proposed by Johnston (1943), and is based upon Kp indices. The second one aims at selecting days that are magnetically quiet or very quiet. Introduced by Mayaud (1973), this is based upon aa indices.

As each month they compulsorily determine 5 quiet and 5 disturbed days., when using quietest and most disturbed days, one should keep in mind that it may happen that during very active periods a selected quietest days is definitely not a quiet day, and that on the contrary during very quiet periods a selected most disturbed days is in fact a quiet day.

Classification of days as deduced from Kp indices

The identification of the quietest and most disturbed days of each month is made on the basis of three criteria:

- The sum of the eight values of Kp;
- The sum of the squares of these values;
- The greatest of the eight values of Kp.

According to each of these criteria, a relative "order number" is assigned to each day of a month, the three order numbers are averaged and the days with the lowest and the highest mean order numbers are selected as the five quietest, the ten quietest (Q-) and the five most disturbed (D-) days.

As already mentioned, it should be noted that these selection criteria give only a relative indication of the character of the selected days with respect to the other days of the same month. As the general disturbance level may be quite different for different years and also for different months of the same year, the selected quietest days of a month may sometimes be rather disturbed or vice versa. In order to indicate such a situation, selected days which do not satisfy certain absolute criteria are marked as follows:

- a selected "quiet day" is considered "not really quiet" and is marked by the letter A if for that day Ap > 6, or marked by the letter K, if Ap < 6, with one Kp value greater than 3 or two Kp values greater than 2+.
- a selected "disturbed day" is considered "not really disturbed" and marked by an asterisk if Ap is lower than 20.
- Classification of days as deduced from aa indices

The identification of the quiet 24-hour intervals is made firstly on the basis of the mean value of aa which must be lower than 13 nT. Then, each individual aa value of the day is represented by a weight p (see Table 1). A day with a mean value of aa < 13nT and for which the sum of weights p, Σp is higher than, or equal to 4 is a quiet day; if Σp is lower than 4, the day is a really quiet day.

The same rules are applied to select the 48-hour quiet or really quiet intervals, with the same limit for the aa mean value (13 nT) and a limit for Σp equal to 6. One must note that in these intervals every local day (0 h to 24 h in local time) is really quiet, at any longitude.

Table 1: the weights p attributed to the aa indices for quiet and very quiet day determination.

p	0	1	2	4	6
aa	<17	17<aa<21	21<aa<28	28<aa<32	>32

Table 2: Correspondance between Kp and Ap

Kp	ap	Kp	ap	Kp	ap
		0o	0	0+	2
1-	3	1o	4	1+	5
2-	6	2o	7	2+	9
3-	12	3o	15	3+	18
4-	22	4o	27	4+	32
5-	39	5o	48	5+	56
6-	67	6o	80	6+	94
7-	111	7o	132	7+	154
8-	179	8o	207	8+	236
9-	300	9o	400		

1.7.2 Global magnetic disturbance : Aa, Am/Km, Ap/Kp

The 3-hour planetary indices aim at characterizing the geomagnetic activity intensity at a planetary level, on the basis of the magnetic activity observed at subauroral latitudes, that is sensitive to the different magnetospheric current sources.

The Kp index was first introduced in 1949. It has since been derived back to 1932 and the present data series is homogeneous and continuous from 1932 onwards. Because of the historical context when Kp was introduced, the Kp network is heavily weighted towards Western Europe and Northern America, where respectively seven and four out of the thirteen stations are located; only two stations are located in the Southern hemisphere and none in Eastern Europe or Asia. Kp behaves as K, and it is therefore not linearly related to the activity. Computing averages of the activity requires an index that is linearly related to the activity. The ap index was therefore introduced few years after. It is expressed in "ap units": 1 ap unit ~ 2 nT. Any ap index is deduced from the corresponding Kp through a one to one correspondence table (see table 2): there is thus only 28 possible ap values. The well known, but generally not properly known, ap index is the daily average of ap; it is expressed also in ap units.

The am index is derived from K-indices measured at a network of subauroral latitude geomagnetic observatories evenly distributed in longitude in both hemispheres. In each hemisphere, stations are gathered in longitude sectors. For each 3-hour interval, hemispheric indices are computed as the weighted average of the K-equivalent amplitudes in the corresponding sectors, and am is the arithmetic average of the two hemispheric indices. The am index is expressed in nT. The present data series is homogeneous from 1959 onwards. An extensive regression analysis of am and solar wind data enabled Svalgaard (1977) to show that any am index is somehow a measure of the energy state of the magnetosphere during the corresponding 3-hour interval.

The 3-hour planetary "aa" antipodal activity index was introduced in order to provide a very long series of geomagnetic activity indices, homogeneous from 1868 onwards. The aa index is a weighted average of the aK equivalent amplitudes from two almost antipodal stations, one in Western Europe, the other in Eastern Australia. The aa index is expressed in nT.

For further details on Kp, aa, and am indices, refer to Mayaud (1980), Menvielle and Berthelier (1991) or to Menvielle et al. (2011).

1.7.3 Magnetic indices related to electric field or current systems: Dst/ SYM-H, AU and AL

Magnetic field measurements are very common, while measurements of electrical currents in both the ionosphere and the magnetosphere are rare. And therefore the variations of the magnetic field are interpreted in terms of electrical currents, as we have previously reported for equivalent electrical currents Sq and EEJ.

Historically, variations in the magnetic field have been used to construct magnetic indices that allow one to approach certain electric currents in the magnetosphere and in the ionosphere.

The northern Polar cap magnetic index is representative for the magnitude of the Northern trans-polar convection electric field which drives the transpolar part of the ionospheric two-cell current system (Stauning, 2012). As a result, increasing PCN values can be interpreted as increasing dayside merging solar wind electric field (see, e.g., Hanuise2006).

The auroral activity AU, AL and AE indices monitor the magnetic activity produced by the auroral electrojets that are mostly related to the magnetosphere-ionosphere coupling through the field-aligned currents: AU monitors the intensity of the electrojet flowing eastward in the Magnetic Local Time (MLT) afternoon sector; AL monitors that of the electrojet flowing westward in the MLT morning sector; AE=AU-AL, AL being negative, is a global indicator that is currently used in substorm activity studies.
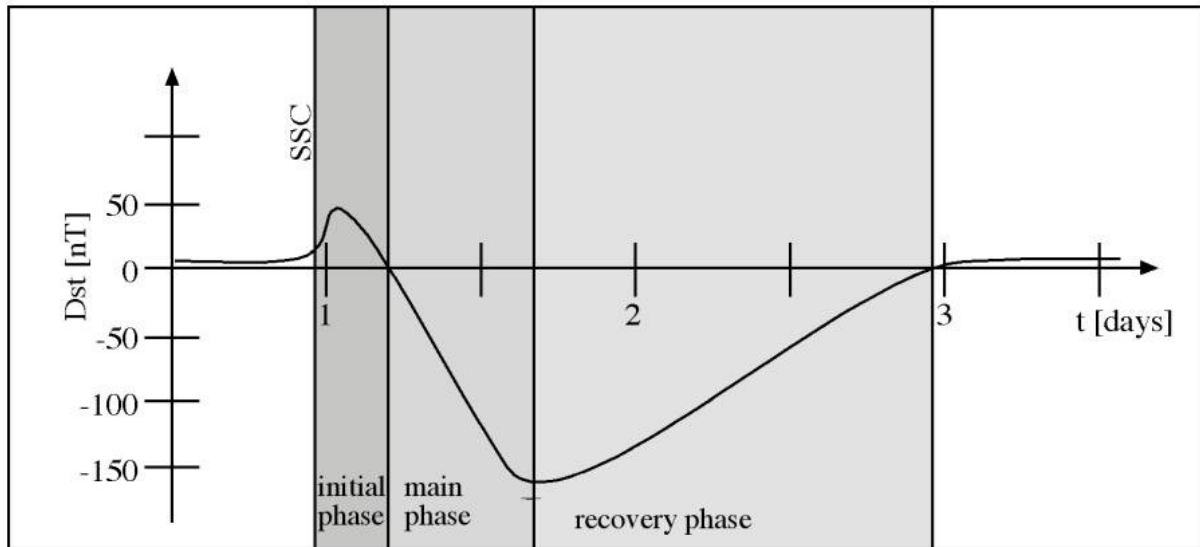
Figure 15 : The Dst index

The Dst index monitors the axi-symmetric part of the magnetospheric currents, including mainly the ring current, but also the magnetopause Chapman-Ferraro current. It is calculated by using magnetic stations of low latitudes located however outside the equatorial electrojet. It presents a positive phase during the compression phase of a magnetic storm and this is due to the electrical currents of the Chapman Ferraro type which circulate on the magnetopause. During the main phase and the magnetic storm it presents a negative signature value of the ring current which develops in the equatorial plane of the magnetosphere (Figure 15). The SYM-H index is mostly similar as the hourly 'Dst' index, but derived from a different set of stations, and with the advantage of being a 1-minute index.

The ASY-H index aims at monitoring the asymmetric part of the low latitude geomagnetic field, in particular during geomagnetic storms. The asymmetric disturbance field has usually been attributed to a partial ring current. However, it may also be interpreted in terms of the effect of a net field-aligned current system flowing into the ionosphere near noon and flowing out near midnight.

Figure 16 : Equatorial Fountain

The reader is referred to Menvielle and Marchaudon (2006) and Menvielle et al. (2011), and references therein for a complete description of geomagnetic indices, and of their physical properties. All of the information c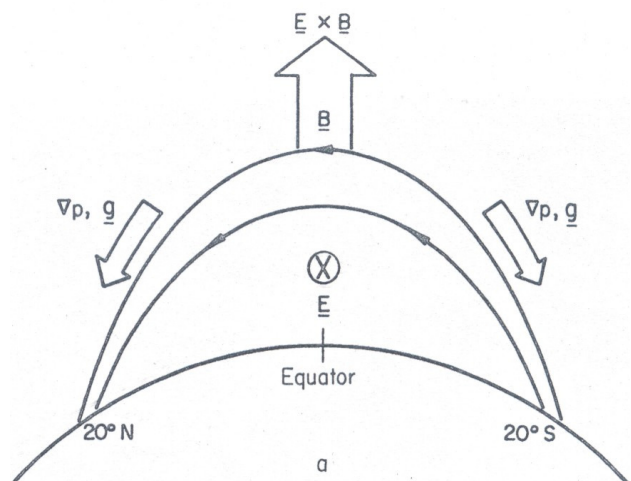oncerning these indices can also be found on the websites: http://isgi.unistra.fr/, and/or http://wdc.kugi.kyoto-u.ac.jp/

1.8 Characteristics of the Equatorial Ionosphere due to B horizontal

1.8.1 Equatorial Fountain

At the magnetic equator the terrestrial magnetic field is horizontal and the plasma is therefore pushed upwards under the effect of the Lorentz force. At higher altitudes the gradients of pressure and gravity influence the movement of ions and electrons ($V_{d//}$: ambipolar diffusion drift) s, and it is in this way that the equatorial fountain represented by figure 16 is formed.

1.8.2 Equatorial Electrojet EEJ

Observations show that the amplitude of the horizontal component of the magnetic field, H, at very low latitudes, is greater than that of the magnetic field at middle latitudes .This is due to the existence of a system of currents, called the Equatorial Electrojet (EEJ), which flows eastward along the magnetic equator in a latitude band of about ±3° on both sides of the magnetic equator. Figure 17, from Jacobs (1990), shows the equatorial electrojet. The increase of the ionospheric electric current at the magnetic equator is due to an increase conductivity related to the geometry. Indeed at the equator the magnetic field B is horizontal.
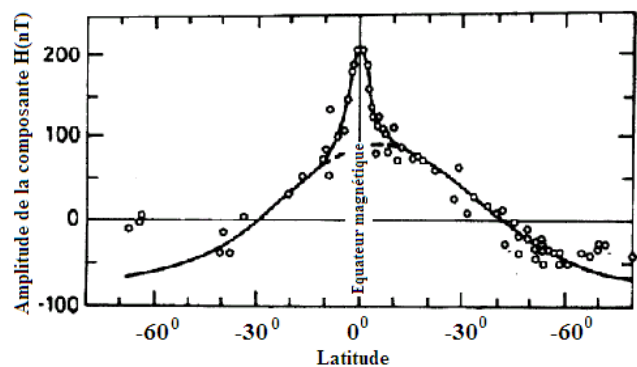

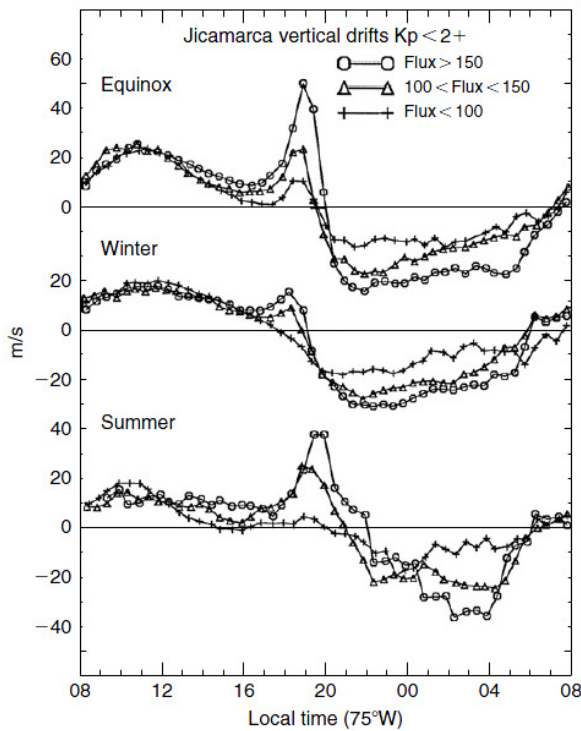Figure 17 : Equatorial Electrojet *EEJ (Jacobs, 1990)*

Figure 18 : Average vertical plasma velocities at Jicamarca during the equinox (March-April, September-October), winter (May-August), summer (November-February) for 3 solar flux values (Fejer et al., 1991)

1.8.3 PRE and plasma bubbles

The drift of the electric field $\vec{E}x\vec{B}$ produces an upwardly directed vertical velocity which causes the ionospheric layers to rise during the day. This velocity is due to an electric field directed towards the east during the day. The vertical velocity is directed downwards, at night this is due to an electric field directed towards the west which produces a descent of the ionosphere towards the lowest altitudes. However, it is observed that between 18.00 and 19.00 LT, the electric field increases before reversing and thus creates a strong increase in vertical speed. Figure 18 from Fejer et al., (1991) presents the vertical velocities observed at Jicamarca in Peru. This phenomenon is called 'Pre Reversal Enhancement', PRE. This figure represents the vertical speed measured by the Jicamarca radar for the 3 seasons (equinox, summer and winter) and for different values of the magnetic index Kp

The strong increase in vertical velocity just after sunset causes a rapid rise of plasma in region F. However, after sunset and in the absence of ionization, the electron density in the F1 region at altitudes lower than 180 km drops rapidly as the loss reactions are rapid. On the contrary, the much longer time constants of the recombination reactions in the F2 region at altitudes above ~ 250 km result in a small change in electron density, which therefore retains much higher values than those of the F1 region, often 2 orders of magnitude. The low-density plasma of the so-called "layer" F1 region is thus located below the "heavy" plasma of high density and the interface between these two media of different density is subject to a type instability Rayleigh - Taylor which creates the "Equatorial Plasma Bubbles", EPB (Kelley, 2009). This instability leads to the formation of very large amplitude irregularities in the ionospheric plasma which affect the electromagnetic signals and cause scintillations on the GPS signal (Basu and Basu, 1981), the appearance of spread F on the ionograms (Abdu et al., 1981; Abdu et al., 1983) and "plumes" on VHF radar observations (Woodman and La Hoz, 1976).

1.8.4 Electrodynamics coupling between high and low latitudes

There are many current systems that affect the auroral zone (Troshichev and Janshura, 2012; Stauning, 2012). In this part we consider only those which extend towards the lower latitudes.

Two main mechanisms are invoked to explain the magnetic disturbances, associated to auroral phenomena and observed at low latitudes during magnetic storms:

1) the prompt penetration of magnetospheric convection electric field (PPEF)

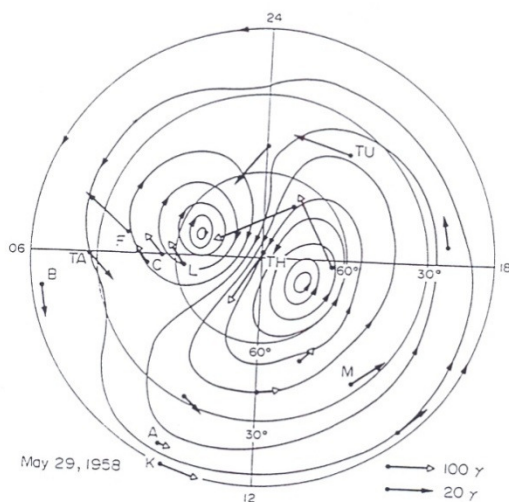2) the ionospheric disturbance dynamo electric field (DDEF)

Figure 19a: DP2 current system (Nishida et al., 1968)

Figure 19b : current system predicted by Blanc and Richmond's model (Mazaudier and Venkateswaran, 1990)

The first mechanism was first revealed by its magnetic signature (Nishida, 1968) and then modeled for the first time by Vasyliunas (1970, 1972). The physical process is the transmission at low latitudes of the electric field associated with magnetospheric convection. The peculiarity of this physical process is that it is observed simultaneously all over the globe. The equivalent current system associated with this physical process is the current DP2. It is composed of 2 current cells. It is shown in figure 19a.
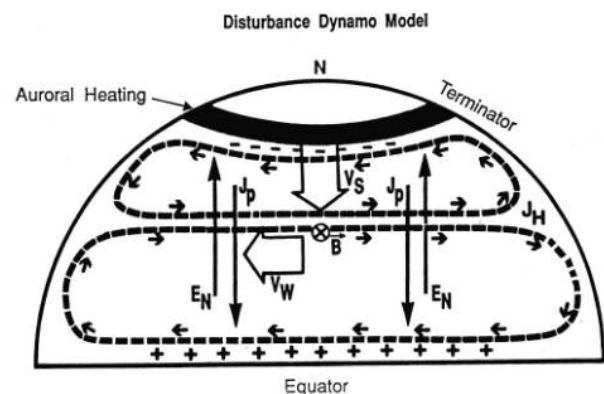
15

The second mechanism, the ionospheric dynamo, was first predicted by the modeling done by Blanc and Richmond (1980). The Joule energy dissipated by the auroral electrojets produces a disturbed circulation of the thermospheric winds which, by dynamo effect, creates ionospheric electric currents. The magnetic signature of the ionospheric disturbance dynamo was first isolated by Le Huy and Amory-Mazaudier (2005) and named D_{dyn}. It is important to note here that before, Fejer et al., (1983) using the incoherent diffusion sounder of Jicamarca had separated the electric field from the magnetospheric convection at the origin of the DP2 (Prompt Penetration Eelctric Field PPEF) from the electric field due to the ionospheric disturbed dynamo at the origin of D_{dyn} (Disturbed Dynamo Electric Field DDFE) . Figure 19b, from Mazaudier and Venkateswaran (1990) represents the current system predicted by Blanc and Richmond (1980). This figure was thus commented by Mazaudier and Venkateswaran:

" *Schematic of the variables in the Blanc-Richmond (1980) theory. The Joule heating from the storm is assumes to extend uniformly around the high-latitude zone. The southward meridional winds at F region heights arising from this heating is shown by the arrow V_s. Due to the action of the Coriolis force, the souhtward meridional winf produces westward motion (shown as the arrow V_w). The zonal motion of the ions in combination with the downward component of the magnetic field (shown as x B) produces an equatorward Pedersen currents (shown as J_p).The Pedersen current builds up positive charges at the equator until an electric field is established in the poleward direction opposing the flow of the Pedersen current. This poleward electric field is shown as E_N. This electric field which is perpendicular to the downward component of B gives rise to an eastward Hall current with maximum intensity in middle latitudes. This Hall current is marked by J_H.The Hall current is interrupted at the terminators and gives rise to two current vortices as shown. The lower latitude disturbance current vortex is opposite in direction to the normal Sq current vortex*".

Mazaudier et al., (1985) measured the perturbed souhtward thermospheric winds (V_s) with amplitude similar to that predicted by Blanc and Richmond (1980) with the incoherent scatter sounder of Saint-Santin. During magnetic storms, the thermal expansion of the atmosphere produces global changes in temperatures, pressures, and atmospheric motions which in turn lead to changes in atmospheric composition (Fuller-Rowell et al., 1994). "*Storm-time composition changes have not been specifically studied by the North-South network of scientists, although this is an active area of research by others.*"

Conclusion

In this Part A, we presented some knowledge essential for the understanding of the ionospheric observations. When analyzing ionospheric data or magnetic field data, it is essential to know the state of the Earth-Sun system and the physical processes acting in the system: a systemic analysis is needed.

The systemic analysis must include at least the following data sets available on the web:
- ✓ data on the phase of the solar cycle (poloidal, toroidal) –**Solar dynamo** -
- ✓ data on current or previous solar events (Solar Flare, CME, HSSW …), it is essential to analyze rather long periods and not few days, see section –**Sun Earth connections** -
- ✓ data of solar wind parameters and especially those governing the solar wind magnetosphere dynamo (B_{imf}, V_{sw}) – **Solar wind/magnetosphere Dynamo** -
- ✓ data on magnetic indices, to understand the magnetospheric and ionospheric electric currents associated to the different dynamos – **Solar dynamo / Solar wind-magnetosphere dynamo/ Ionospheric disturbed dynamo** -
- ✓ data on the atmosphere which is the main engine of the ionospheric dynamo (B, V_n), -**regular ionospheric dynamo**-
- ✓ data of the magnetometer networks which allow to evaluate the geographical impact of the different physical processes at work in the Sun Earth system by their magnetic disturbance **- equivalent electric current systems**-

Figure 20 summarizes what we presented in this tutorial. From top to bottom there are the Sun with its two poloidal and toroiodal (sunspot) magnetic components, the magnetosphere, the ionosphere, the layers of the atmosphere and the interior of the earth. The four permanent dynamos are highlighted in yellow.

There are secondary dynamos NP dynamo (NP: non permanent) occurring during geomagnetic cativity: 1) one inside the magnetosphere which converts the motion of particles in ring current and 2) and one inside the ionosphere related to the storm thermospheric winds related to Joule heating dissipation in the auroral zone.

On the right of the figure we have represented the radiation channel and on the left the solar wind channel. The EUV, UV and X radiations act directly on the ionosphere (photo ionization), and on the atmosphere (creation of the migrating tides in the stratosphere). Visible and infrared radiations reach the ground. In the troposphere, atmospheric convection produces non-migrating tides. Migrating and non-migrating tides propagate to higher altitude where they participate in the ionospheric dynamo.

We have drawn by dashed lines in green the perturbations which exist during magnetic activity. There are Solar Flares (radiation disturbances) and solar wind perturbations associated with CME and HSSW. The regular solar wind acts continually on the magnetosphere, but its action is confined to high latitudes. During magnetic disturbances there is a coupling between high and low latitudes (horizontal lines) following two main processes PPEF and DDEF. In each of the boxes we have noted the equivalent indices and currents associated with the different dynamos. At ground level there are variations of magnetic field B and Ground Induced current, induced by the external electric currents.

We do not claim that this figure presents of all physical processes. We present only those that we can study with the data we have used in our network.

In the part B of this paper we will present the results and capacity building developed in our network.
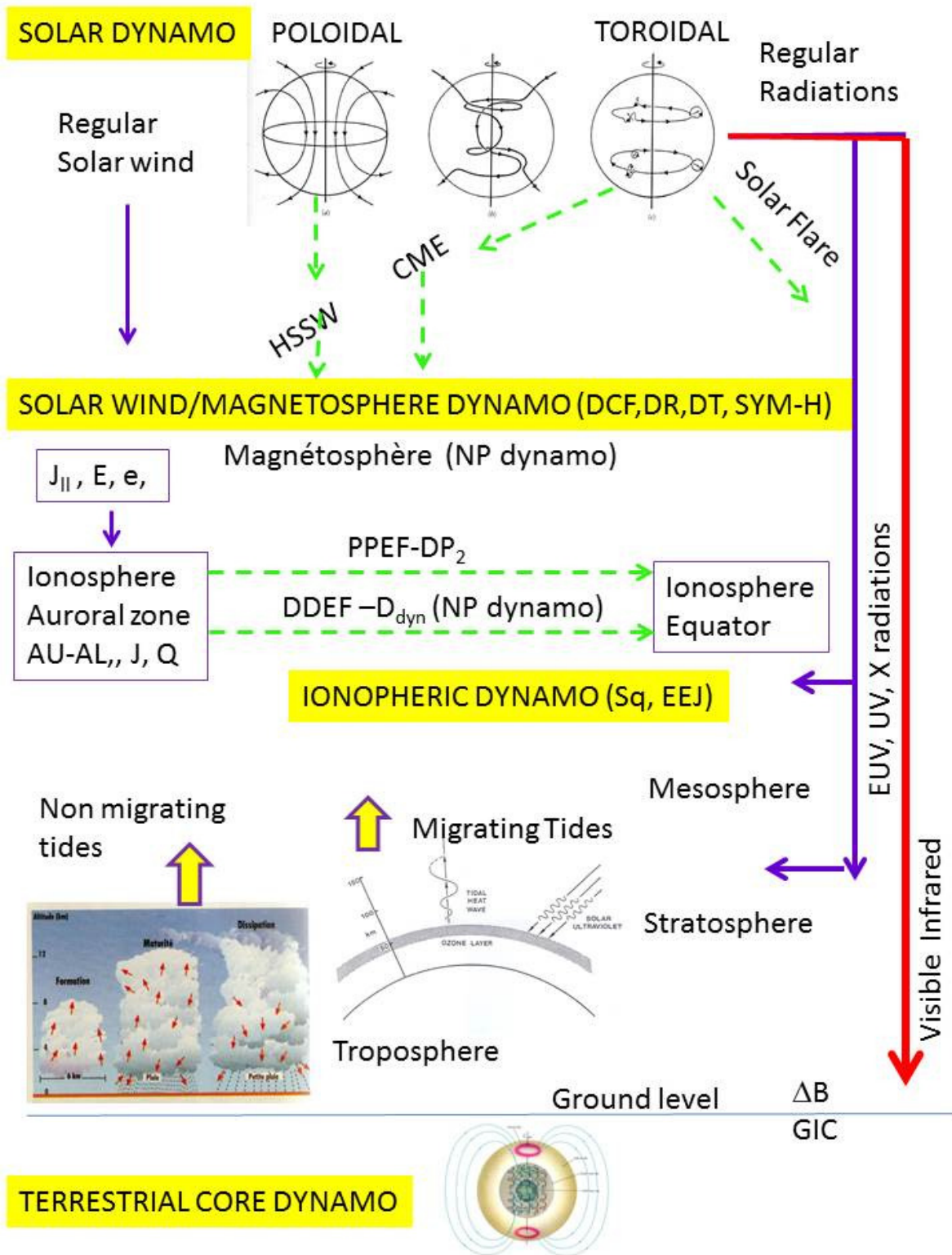
Acknowledgement

Figure 20 : Synthetic diagram

References

M.A. Abdu, I.S. Batista, J.A. Bittencourt, J. A., Some characteristics of spread F at the magnetic equatotorial station Foraleza , J. Geophys. Res., 86, A8 (1981) pp. 6836-6842.

M.A. Abdu, R.T. de Medeiros, J. H. A. Sobral, J.A. Bittencourt, Spread F plasma bubble vertical rise velocities determined from space ionosonde observations, J. Geophys. Res., 88, A11(1983) pp. 9197-9204.

S-I. Akasofu, A model, in Solar Terrestrial Physics, Proc. of the symposium of Solar Terrestrial Physics, Leningrad, USSR 12-19 May, 1970 edited by E.R. Dyer and J.G Roederer, pp. 131-151. (1972) pp. 131-151.

C. Amory-Mazaudier, A. Kobea, P. Vila, A. Achy-Seka, E. Blanc, at al., On Equatorial geophysics studies: The IGRGEA results during the last decade, J. Atmos. Sol. Terres. Phys., 67, 4(2005) pp. 301-313.

C. Amory-Mazaudier, M. Le Huy, Y. Cohen, V. Doumouya, A. Bourdillon, at al., Sun Earth System Interactions over Vietnam: an international cooperative project , Ann. Geophys., 24 (2006) pp. 3313-3327.

C. Amory-Mazaudier, S. Basu, O; Bock, A. Combrink, K. Groves, at al., International Heliophysical Year, GPS network in Africa, Brief report , J. Earth Moon and Planets (2009) doi: 10.1007/s11038-008-9273-8 February.

C. Amory-Mazaudier, R. Fleury, Sh. Gadimiva, Space Weather, from the Sun to the Earth, the key role of GNSS, Coordinates, 2017, 13(2) https://hal.archives-ouvertes.fr/hal-01489731/document

J.C. Amstrong, A.J. Zmuda, aligned current at 1100 Km in the auroral region measured by satellite, J. Geophys. Res. 75 (1970) pp. 7122-7127.

W.I. Axford, C.O. Hines, A Unifying theory of high latitudes geophysical phenomena and geomagnetic storms, Can. J. Phys., 39 (1961) p. 1433.

S. Basu, S. Basu, Equatorial scintillations, a review, J. Atmos. Sol. Terr. Phys., 43, 5/6 (1981) pp. 473-49.

K. Birkeland, The Norvegian aurora polaries expedition, 1902-1903, Aschlovg, Christania, Norvège (1908).

K. Birkeland, The Norvegian aurora polaries expedition, 1902-1903, Aschlovg, Christania, Norvège (1913)

M. Blanc, A.D. Richmond, The ionospheric disturbance dynamo, J. Geophys. Res., 85, A4 (1980), pp. 1669-1686, doi: 10.1029/JA085iA04p01669

J. Casanovas, The discovery of sunspots, In Historical events and people. Ed. W. Schröder, ISSN-1615-2824, AKGGP/SHGGCP, science Edition Bremen/Postdam (2006) pp. 243-260.

S. Chapman, V.C.A. Ferraro, New theory of magnetic storms, Terr. Magn. Atm. Elec., 36 (1931), p. 77.

S. Chapman, J. Bartels, Geomagnetism (Vol1& 2), Oxford University Press (1940).

S. Chapman, Equatorial electrojet as detected from the abnormal electric current distribution above Huancayo, Peru, and elsewhere, Arch. Meteorol. Geophys., 4, (1951) pp. 368-390.

S. Chapman, R.S. Lindzen, Atmospheric tides: thermal and gravitational, D. Reidel publishing company/ Dordrecht, Hollande (1970).

J-J. Curto, C. Amory-Mazaudier, M. Menvielle, J.M. Torta, Study of Solar Flare Effects at Ebre: 1. Regular and reversed SFe, Statistical analysis (1953, 1985) and a global case study, J. Geophys. Res., 99, A3 (1994a) pp. 3945-3954.

J-J. Curto, C. Amory-Mazaudier, J.M. Torta, M. Menvielle, Study of Solar Flare Effects at Ebre: 2. Unidimensional physical integrated model, J. Geophys. Res., A12 (1994b) pp. 23289-23296.

V. Doumouya, J. Vassal, Y. Cohen, O. Fambitakoye, M. Menvielle, Equatorial electrojet at African longitudes: first results from magnetic measurements, Ann. Geophys., 16, (1997) pp. 677-697.

J. Ducruix, V. Courtillot, V., J.L. Le Mouël, Induction effects associated with the equatorial electrojet, J. Geophys. Res., 82 (1997) pp. 335-351.

T.W. Dungey, Interplanetary magnetic field and the auroral zones, Phys. Rev. Lett. 6 (1961), pp. 47.

J.V. Evans, Incoherent scatter contributions to studies of the dynamics of the lower thermosphere, Rev. Geophys. Space Phys, Rev. Geophys. Space Phys, 16 (1978) pp. 195.

O. Fambitakoye, P.N. Mayaud, The Equatorial electrojet and regular daily variation SR - I. A determination of the equatorial electrojet parameters, J. Atmos. Terr. Phys., 38 (1976) pp. 1-17.

O. Fambitakoye, Étude des effets magnétiques de l'Electrojet équatorial, Thèse d'État. ORSTOM (1976). ISBN 2-7099-408-X .

B.G. Fejer, M.F. Larsen, D.T. Tarpley, Equatorial Disturbances Dynamo Electric Fiels, Geophys. Res. Lett., 10, 7 (1973) pp. 537-540.

B.G. Fejer, E.R. Depaula, S.A. Gonzalez, R.F. Woodman, Average vertical and zonal F region plasma drifts over Jicamarca, J. Geophys. Res., 96, A8 (1991) pp. 13,901-13,906.

T.J. Fuller-Rowell, M. V. Codrescu, R. J. Moffett, S. Quegan, Response of the thermosphere and ionosphere to geomagnetic storms, J. Geophys. Res., 99, A3 (1994) pp. 3893- 3914. doi:10.1029/93JA02015.

W.D. Gonzalez, J.A. Joselyn, Y. Kamide, H.W. Kroehl, G. Rostoker, B.T. Tsurutani, V.M. Vasyliunas, What is a geomagnetic storm ? J. Geophys. Res., 99, A4, (1994) pp. 5771-5792.

N. Goplaswamy, Coronal Mass Ejection, A summary of recent results, Proc. of the 20th Slovak National Solar Physics Workshop, Ed; I Dorotovic, Slovak Central Observatory (2010) pp. 108- 130.

M.E. Hagan, J.M. Forbes, Migrating and nonmigrating diurnal tides in the middle and upper atmosphere excited by tropospheric latent heat release, J. Geophys. Res., 107, D24 (2002) pp. 4754. doi:10.1029/ 2001JD001236.

M.E. Hagan, J.M. Forbes, Migrating and nonmigrating semidiurnal tides in the upper atmosphere excited by tropospheric latent heat release, J. Geophys. Res., 108, A2 (2003) pp 1062. doi:10.1029/2002JA009466.

G.E. Hale, F. Ellerman, S.B. Nicholson, A.H. Joy, The Magnet ic Polarity of Sun-Spots , Astrophys. J., 49 (1919) pp. 153, doi:10.1086/142452

C. Hanuise, J.C. Cerisier, F. Auchere, K. Bocchialini, S. Bruinsma, at al., Impact of the 26-30 May 2003 solar events on the earth ionosphere and thermosphere Ann. Geophys., 24 (2006) pp. 129-151.

R. Harrison, A. Breen, B. Bromage, J. Davila, International Heliophysical Year Astronomy & Geophysics, 46, (2005) pp. 327 .

R. Hutton, Some problems of electromagnetic induction in the Equatorial Electrojet region - 1 magneto-telluric relations, Geophys. J. R. astr. Soc., 28 (1972) pp. 267-284.

J.A. Jacobs, Geomagnetism. Academic Press, London (1990).

H.F. Johnston, Mean K-indices from twenty one magnetic observatories and five quiet and five disturbed days for 1942, Terr. Magn. Atmos. Elec., 47 (1943) pp. 219.

A. Kavanagh, M. Denton, High-speed solar-wind streams and Geospace interactions, A&G, 48, 6 (2007) pp 24. doi: 10.1111/j.1468-4004.2007.48624.x

Kitamura,M., D. Wentzel, A.A. Henden, J. Bennett, H.M.K Al-Naimiy, at al., The United Nations Basic Space Science Initiative : The TRIPOD concept, Proc. IAU symp. 2007, International Astronomical Union (2007).

M.C. Kelley, the Earth Ionosphere, Academic Press, San Diego (1989).

J-P. Legrand, P. Simon, A review for geophysicists: Part I : The contribution to geomagnetic activitu of shock waves and of the solar wind, Ann. Geophys., 7, 6, (1989) pp 565-578.

J-P. Legrand, Introduction élémentaire à la physique cosmique et à la physique des relations Terre-Soleil. Ed. CNRS-INAG (1984).

M. Le Huy, C. Amory-Mazaudier, Magnetic signature of the ionospheric disturbance dynamo at equatorial latitudes: "Ddyn", J. Geophys. Res., 110, A10301 (2005). doi:10.1029/2004JA010578.

H. Luu Viet, M. Menvielle, M. Le Huy, Proceedings of the 2nd International Conference on Green Technology and Sustainable Development, Dhaka/Bamgladesh, 5-6 September (2014) pp 26 – 34.

S. Macmillan, C. Finlay , The International Geomagnetic Reference Field, in Geomagnetic Observations and Models, M. Mandea and M. Korten (eds.), IAGA Special Sopron Book Series, 5 (2011) pp 265. doi: 10.1007/978-90-481-9858-08, Springer.

P.N. Mayaud, A hundred series of Geomagnetic data 1868-1967, indices aa, Storm sudden commencements, AIGA Bulletin n°33, IUGG Publication Office (1973) pp252, Paris.

P.N. Mayaud, Derivation, meaning, and use of geomagnetic indices, Geophys. Monogr. Ser., vol. 22, AGU, Washington, D.C (1980).

C. Mazaudier, R. Bernard, S. Venkateswaran, Saint-Santin radar observations of lower thermospheric storms, J. Geophys. Res., 90, A3 (1985) pp. 2885-2895, correction: J. Geophys. Res., 90 , A7 (1985) pp. 6685-6686.

C. Mazaudier, S.V. Venkateswaran, Delayed ionospheric effects of March 22, 1979 studied by the sixth Coordinated Data Analysis Workshop (CDAW-6), Ann. Geophys., 8, (1990) pp. 511-518.

C. Mazaudier, J. Achache, A. Achy-Seka, E. Albouy, E. Blanc, at al., International Equatorial Electrojet Year, Brazilian J. Geophys. 11, 3 (1993) pp. 303-317, special issue.

M. Menvielle, A. Berthelier, The K-derived planetary indices: description and availability, Rev. Geophys. Space Phys., 29 (1991) pp. 415-432; erratum: 30 (1992) pp 91.

M. Menvielle, A. Marchaudon,Geomagnetic indices in Solar-Terrestrial Physics and Space Weather, /in/Space Weather, J. Lilensten (ed.), Springer, 277 (2006).

M. Menvielle, T. Iyemori, A. Marchaudon, M. Nose, Geomagnetic indices , *in* Geomagnetic Observations and Models, M. Mandea, M. Korte (eds.), Geomagnetic indices, Special Sopron Book Series 5, Springer, Dordrecht Heidelberg London New York, (2011). doi: 10.1007/978-90-481-9858-08.

Nishida, Geomagnetic DP2 fluctuations and associated magnetospheric phenomena, J. Geophys. Res., 73, (1968) pp. 1795-1803. doi: 10.1029/JA073i005p01795.

L. Paterno, History of solar cycle, in Historical events and people, W. Schröder, ISSN-1615-2824, AKGGP/SHGGCP, science Edition Bremen/Postdam (2005) pp. 261-275.

W.R. Peltier, J-F. Hermance, Magnetotelluric fields of a Gaussian electrojet, Can. J. Earth Sci., 8, (1971) 338-346.

A. Richmond, Ionospheric Electrodynamics , in Atmospheric Electrodynamics, Vol II, Chapter 9 (1995) pp 249-280, Edited by Hans Volland.

H. Rishbeth, O.K. Gariott, Introduction to Ionospheric Physics. International Geophys. Ser., 14, Ed Academic Press (1969) 344 pages , ISBN 0125889402

H. Schwabe, Beobachtungen im Jahre, Astron. Nachr. 21 (1843) pp. 234–235. doi:10.1002/asna.18440211505

P. A. Simon, J-P. Legrand, A review for Geophysicists, Part II The solar sources of geomagnetic activitu and their lins with sunspot cycle activity, Ann. Geophys., 7, 6 (1989) pp 579-594.

P. Stauning, The Polar Cap PC Indices: Relations to Solar Wind and Global Disturbances, In Exploring the Solar Wind, Dr. Marian Lazar (Ed.),(2012) ISBN: 978-953-51-0339-4, *InTech*,

C. Störmer, Sur les trajectoires des corpuscules électrisées dans l'espace sous l'action du magnétisme terrestre avec application aux aurores boréales, Arch. Sci. Phys. Genève , 24 (1907) pp (5, 113, 121, 317).

C. Störmer, Sur les trajectoires des corpuscules électrisées dans l'espace sous l'action du magnétisme terrestre avec application aux aurores boréales, Arch. Sci. Phys. Genève, 32, 33 (1911)163 pp.

C. Störmer, Sur les trajectoires des corpuscules électrisées dans l'espace sous l'action du magnétisme terrestre avec application aux aurores boréales, Arch. Sci. Phys. Genève, 35 (1913) pp 483-8.

O. Troshichev, A. Janshura, In Space weather Monitoring by Ground-based Means PC index, 23 (2012) pp 127. http://www.springer.com/978-3-642-16802-4.

L. Svalgaard, Geomagnetic activity: Dependence on solar wind parameters, in Skylab Workshop Monograph on Coronal Holes, edited by J. B. Zirker, chap. 9, (1977) p. 371, Columbia Univ. Press, New York.

J. Vassal, M. Menvielle, M. Dukhan, K. Boka, Y. Cohen, V. Doumouya, O. Fambitakoye, A study of the transient variations of the Earth electromagnetic field at dip latitudes in Western Africa (Mali and Côte d'Ivoire), Ann. Geophys., 16 (1998) pp. 658-676.

V.M. Vasyliunas, Mathematical models of magnetospheric convection and its coupling to the ionosphere in *Particles and Fields in the Magnetosphere*, edited by B.M. McCormac, Springer, New York (1970) pp. 60-71.

V.M. Vasyliunas, The inter-relationship of magnetospheric processes, in *Earth's Magnetosphere Processes*, edited by M. McCormac Springer, New York (1972) pp. 29-38.

R.F. Woodman, C. La Hoz, Radar Observations of the F region equatorial irregularities, J. Geophys. Res., 81 (1976) pp. 5447-5466.